

Measurement of the B_s^0 - \bar{B}_s^0 Oscillation Frequency

A. Abulencia,²³ D. Acosta,¹⁷ J. Adelman,¹³ T. Affolder,¹⁰ T. Akimoto,⁵⁵ M.G. Albrow,¹⁶ D. Ambrose,¹⁶ S. Amerio,⁴³ D. Amidei,³⁴ A. Anastassov,⁵² K. Anikeev,¹⁶ A. Annovi,¹⁸ J. Antos,¹ M. Aoki,⁵⁵ G. Apollinari,¹⁶ J.-F. Arguin,³³ T. Arisawa,⁵⁷ A. Artikov,¹⁴ W. Ashmanskas,¹⁶ A. Attal,⁸ F. Azfar,⁴² P. Azzi-Bacchetta,⁴³ P. Azzurri,⁴⁶ N. Bacchetta,⁴³ H. Bachacou,²⁸ W. Badgett,¹⁶ A. Barbaro-Galtieri,²⁸ V.E. Barnes,⁴⁸ B.A. Barnett,²⁴ S. Baroiant,⁷ V. Bartsch,³⁰ G. Bauer,³² F. Bedeschi,⁴⁶ S. Behari,²⁴ S. Belforte,⁵⁴ G. Bellettini,⁴⁶ J. Bellinger,⁵⁹ A. Belloni,³² E. Ben Haim,⁴⁴ D. Benjamin,¹⁵ A. Beretvas,¹⁶ J. Beringer,²⁸ T. Berry,²⁹ A. Bhatti,⁵⁰ M. Binkley,¹⁶ D. Bisello,⁴³ R. E. Blair,² C. Blocker,⁶ B. Blumenfeld,²⁴ A. Bocci,¹⁵ A. Bodek,⁴⁹ V. Boisvert,⁴⁹ G. Bolla,⁴⁸ A. Bolshov,³² D. Bortoletto,⁴⁸ J. Boudreau,⁴⁷ A. Boveia,¹⁰ B. Brau,¹⁰ C. Bromberg,³⁵ E. Brubaker,¹³ J. Budagov,¹⁴ H.S. Budd,⁴⁹ S. Budd,²³ K. Burkett,¹⁶ G. Busetto,⁴³ P. Bussey,²⁰ K. L. Byrum,² S. Cabrera,¹⁵ M. Campanelli,¹⁹ M. Campbell,³⁴ F. Canelli,⁸ A. Canepa,⁴⁸ D. Carlsmith,⁵⁹ R. Carosi,⁴⁶ S. Carron,¹⁵ B. Casal,¹¹ M. Casarsa,⁵⁴ A. Castro,⁵ P. Catastini,⁴⁶ D. Cauz,⁵⁴ M. Cavalli-Sforza,³ A. Cerri,²⁸ L. Cerrito,⁴² S.H. Chang,²⁷ J. Chapman,³⁴ Y.C. Chen,¹ M. Chertok,⁷ G. Chiarelli,⁴⁶ G. Chlachidze,¹⁴ F. Chlebana,¹⁶ I. Cho,²⁷ K. Cho,²⁷ D. Chokheli,¹⁴ J.P. Chou,²¹ P.H. Chu,²³ S.H. Chuang,⁵⁹ K. Chung,¹² W.H. Chung,⁵⁹ Y.S. Chung,⁴⁹ M. Ciljak,⁴⁶ C.I. Ciobanu,²³ M.A. Ciocci,⁴⁶ A. Clark,¹⁹ D. Clark,⁶ M. Coca,¹⁵ G. Compostella,⁴³ M.E. Convery,⁵⁰ J. Conway,⁷ B. Cooper,³⁰ K. Copic,³⁴ M. Cordelli,¹⁸ G. Cortiana,⁴³ F. Crescioli,⁴⁶ A. Cruz,¹⁷ C. Cuenca Almenar,⁷ J. Cuevas,¹¹ R. Culbertson,¹⁶ D. Cyr,⁵⁹ S. DaRonco,⁴³ S. D'Auria,²⁰ M. D'Onofrio,³ D. Dagenhart,⁶ P. de Barbaro,⁴⁹ S. De Cecco,⁵¹ A. Deisher,²⁸ G. De Lentdecker,⁴⁹ M. Dell'Orso,⁴⁶ F. Delli Paoli,⁴³ S. Demers,⁴⁹ L. Demortier,⁵⁰ J. Deng,¹⁵ M. Deninno,⁵ D. De Pedis,⁵¹ P.F. Derwent,¹⁶ G.P. Di Giovanni,⁴⁴ B. Di Ruzza,⁵⁴ C. Dionisi,⁵¹ J.R. Dittmann,⁴ P. DiTuro,⁵² C. Dörr,²⁵ S. Donati,⁴⁶ M. Donega,¹⁹ P. Dong,⁸ J. Donini,⁴³ T. Dorigo,⁴³ S. Dube,⁵² K. Ebina,⁵⁷ J. Efron,³⁹ J. Ehlers,¹⁹ R. Erbacher,⁷ D. Errede,²³ S. Errede,²³ R. Eusebi,¹⁶ H.C. Fang,²⁸ S. Farrington,²⁹ I. Fedorko,⁴⁶ W.T. Fedorko,¹³ R.G. Feild,⁶⁰ M. Feindt,²⁵ J.P. Fernandez,³¹ R. Field,¹⁷ G. Flanagan,⁴⁸ L.R. Flores-Castillo,⁴⁷ A. Foland,²¹ S. Forrester,⁷ G.W. Foster,¹⁶ M. Franklin,²¹ J.C. Freeman,²⁸ H. J. Frisch,¹³ I. Furic,¹³ M. Gallinaro,⁵⁰ J. Galyardt,¹² J.E. Garcia,⁴⁶ M. Garcia Sciveres,²⁸ A.F. Garfinkel,⁴⁸ C. Gay,⁶⁰ H. Gerberich,²³ D. Gerdes,³⁴ S. Giagu,⁵¹ P. Giannetti,⁴⁶ A. Gibson,²⁸ K. Gibson,¹² C. Ginsburg,¹⁶ N. Giokaris,¹⁴ K. Giolo,⁴⁸ M. Giordani,⁵⁴ P. Giromini,¹⁸ M. Giunta,⁴⁶ G. Giurgiu,¹² V. Glagolev,¹⁴ D. Glenzinski,¹⁶ M. Gold,³⁷ N. Goldschmidt,³⁴ J. Goldstein,⁴² G. Gomez,¹¹ G. Gomez-Ceballos,¹¹ M. Goncharov,⁵³ O. González,³¹ I. Gorelov,³⁷ A.T. Goshaw,¹⁵ Y. Gotra,⁴⁷ K. Goulios,⁵⁰ A. Gresele,⁴³ M. Griffiths,²⁹ S. Grinstein,²¹ C. Grosso-Pilcher,¹³ R.C. Group,¹⁷ U. Grundler,²³ J. Guimaraes da Costa,²¹ Z. Gunay-Unalan,³⁵ C. Haber,²⁸ S.R. Hahn,¹⁶ K. Hahn,⁴⁵ E. Halkiadakis,⁵² A. Hamilton,³³ B.-Y. Han,⁴⁹ J.Y. Han,⁴⁹ R. Handler,⁵⁹ F. Happacher,¹⁸ K. Hara,⁵⁵ M. Hare,⁵⁶ S. Harper,⁴² R.F. Harr,⁵⁸ R.M. Harris,¹⁶ K. Hatakeyama,⁵⁰ J. Hauser,⁸ C. Hays,¹⁵ A. Heijboer,⁴⁵ B. Heinemann,²⁹ J. Heinrich,⁴⁵ M. Herndon,⁵⁹ D. Hidas,¹⁵ C.S. Hill,¹⁰ D. Hirschbuehl,²⁵ A. Hocker,¹⁶ A. Holloway,²¹ S. Hou,¹ M. Houlden,²⁹ S.-C. Hsu,⁹ B.T. Huffman,⁴² R.E. Hughes,³⁹ J. Huston,³⁵ J. Incandela,¹⁰ G. Introzzi,⁴⁶ M. Iori,⁵¹ Y. Ishizawa,⁵⁵ A. Ivanov,⁷ B. Iyutin,³² E. James,¹⁶ D. Jang,⁵² B. Jayatilaka,³⁴ D. Jeans,⁵¹ H. Jensen,¹⁶ E.J. Jeon,²⁷ S. Jindariani,¹⁷ M. Jones,⁴⁸ K.K. Joo,²⁷ S.Y. Jun,¹² T.R. Junk,²³ T. Kamon,⁵³ J. Kang,³⁴ P.E. Karchin,⁵⁸ Y. Kato,⁴¹ Y. Kemp,²⁵ R. Kephart,¹⁶ U. Kerzel,²⁵ V. Khotilovich,⁵³ B. Kilminster,³⁹ D.H. Kim,²⁷ H.S. Kim,²⁷ J.E. Kim,²⁷ M.J. Kim,¹² S.B. Kim,²⁷ S.H. Kim,⁵⁵ Y.K. Kim,¹³ L. Kirsch,⁶ S. Klimenko,¹⁷ M. Klute,³² B. Knuteson,³² B.R. Ko,¹⁵ H. Kobayashi,⁵⁵ K. Kondo,⁵⁷ D.J. Kong,²⁷ J. Konigsberg,¹⁷ A. Korytov,¹⁷ A.V. Kotwal,¹⁵ A. Kovalev,⁴⁵ A. Kraan,⁴⁵ J. Kraus,²³ I. Kravchenko,³² M. Kreps,²⁵ J. Kroll,⁴⁵ N. Krumnack,⁴ M. Kruse,¹⁵ V. Krutelyov,⁵³ S. E. Kuhlmann,² Y. Kusakabe,⁵⁷ S. Kwang,¹³ A.T. Laasanen,⁴⁸ S. Lai,³³ S. Lami,⁴⁶ S. Lammel,¹⁶ M. Lancaster,³⁰ R.L. Lander,⁷ K. Lannon,³⁹ A. Lath,⁵² G. Latino,⁴⁶ I. Lazzizzera,⁴³ T. LeCompte,² J. Lee,⁴⁹ J. Lee,²⁷ Y.J. Lee,²⁷ S.W. Lee,⁵³ R. Lefèvre,³ N. Leonardo,³² S. Leone,⁴⁶ S. Levy,¹³ J.D. Lewis,¹⁶ C. Lin,⁶⁰ C.S. Lin,¹⁶ M. Lindgren,¹⁶ E. Lipeles,⁹ T.M. Liss,²³ A. Lister,¹⁹ D.O. Litvintsev,¹⁶ T. Liu,¹⁶ N.S. Lockyer,⁴⁵ A. Loginov,³⁶ M. Loreti,⁴³ P. Loverre,⁵¹ R.-S. Lu,¹ D. Lucchesi,⁴³ P. Lujan,²⁸ P. Lukens,¹⁶ G. Lungu,¹⁷ L. Lyons,⁴² J. Lys,²⁸ R. Lysak,¹ E. Lytken,⁴⁸ P. Mack,²⁵ D. MacQueen,³³ R. Madrak,¹⁶ K. Maeshima,¹⁶ T. Maki,²² P. Maksimovic,²⁴ S. Malde,⁴² G. Manca,²⁹ F. Margaroli,⁵ R. Marginean,¹⁶ C. Marino,²³ A. Martin,⁶⁰ V. Martin,³⁸ M. Martínez,³ T. Maruyama,⁵⁵ P. Mastrandrea,⁵¹ H. Matsunaga,⁵⁵ M.E. Mattson,⁵⁸ R. Mazini,³³ P. Mazzanti,⁵ K.S. McFarland,⁴⁹ P. McIntyre,⁵³ R. McNulty,²⁹ A. Mehta,²⁹ S. Menzemer,¹¹ A. Menzione,⁴⁶ P. Merkel,⁴⁸ C. Mesropian,⁵⁰ A. Messina,⁵¹ M. von der Mey,⁸ T. Miao,¹⁶ N. Miladinovic,⁶ J. Miles,³² R. Miller,³⁵ J.S. Miller,³⁴ C. Mills,¹⁰ M. Milnik,²⁵ R. Miquel,²⁸ A. Mitra,¹ G. Mitselmakher,¹⁷ A. Miyamoto,²⁶ N. Moggi,⁵ B. Mohr,⁸

R. Moore,¹⁶ M. Morello,⁴⁶ P. Movilla Fernandez,²⁸ J. Mülmenstädt,²⁸ A. Mukherjee,¹⁶ Th. Müller,²⁵ R. Mumford,²⁴ P. Murat,¹⁶ J. Nachtman,¹⁶ J. Naganoma,⁵⁷ S. Nahn,³² I. Nakano,⁴⁰ A. Napier,⁵⁶ D. Naumov,³⁷ V. Necula,¹⁷ C. Neu,⁴⁵ M.S. Neubauer,⁹ J. Nielsen,²⁸ T. Nigmanov,⁴⁷ L. Nodulman,² O. Norniella,³ E. Nurse,³⁰ T. Ogawa,⁵⁷ S.H. Oh,¹⁵ Y.D. Oh,²⁷ T. Okusawa,⁴¹ R. Oldeman,²⁹ R. Orava,²² K. Osterberg,²² C. Pagliarone,⁴⁶ E. Palencia,¹¹ R. Paoletti,⁴⁶ V. Papadimitriou,¹⁶ A.A. Paramonov,¹³ B. Parks,³⁹ S. Pashapour,³³ J. Patrick,¹⁶ G. Pauletta,⁵⁴ M. Paulini,¹² C. Paus,³² D.E. Pellett,⁷ A. Penzo,⁵⁴ T.J. Phillips,¹⁵ G. Piacentino,⁴⁶ J. Piedra,⁴⁴ L. Pinera,¹⁷ K. Pitts,²³ C. Plager,⁸ L. Pondrom,⁵⁹ X. Portell,³ O. Poukhov,¹⁴ N. Pounder,⁴² F. Prakoshyn,¹⁴ A. Pronko,¹⁶ J. Proudfoot,² F. Ptohos,¹⁸ G. Punzi,⁴⁶ J. Pursley,²⁴ J. Rademacker,⁴² A. Rahaman,⁴⁷ A. Rakitin,³² S. Rappoccio,²¹ F. Ratnikov,⁵² B. Reisert,¹⁶ V. Rekovic,³⁷ N. van Remortel,²² P. Renton,⁴² M. Rescigno,⁵¹ S. Richter,²⁵ F. Rimondi,⁵ L. Ristori,⁴⁶ W.J. Robertson,¹⁵ A. Robson,²⁰ T. Rodrigo,¹¹ E. Rogers,²³ S. Rolli,⁵⁶ R. Roser,¹⁶ M. Rossi,⁵⁴ R. Rossin,¹⁷ C. Rott,⁴⁸ A. Ruiz,¹¹ J. Russ,¹² V. Rusu,¹³ H. Saarikko,²² S. Sabik,³³ A. Safonov,⁵³ W.K. Sakumoto,⁴⁹ G. Salamanna,⁵¹ O. Saltó,³ D. Saltzberg,⁸ C. Sanchez,³ L. Santi,⁵⁴ S. Sarkar,⁵¹ L. Sartori,⁴⁶ K. Sato,⁵⁵ P. Savard,³³ A. Savoy-Navarro,⁴⁴ T. Scheidle,²⁵ P. Schlabach,¹⁶ E.E. Schmidt,¹⁶ M.P. Schmidt,⁶⁰ M. Schmitt,³⁸ T. Schwarz,³⁴ L. Scodellaro,¹¹ A.L. Scott,¹⁰ A. Scribano,⁴⁶ F. Scuri,⁴⁶ A. Sedov,⁴⁸ S. Seidel,³⁷ Y. Seiya,⁴¹ A. Semenov,¹⁴ L. Sexton-Kennedy,¹⁶ I. Sfiligoi,¹⁸ M.D. Shapiro,²⁸ T. Shears,²⁹ P.F. Shepard,⁴⁷ D. Sherman,²¹ M. Shimojima,⁵⁵ M. Shochet,¹³ Y. Shon,⁵⁹ I. Shreyber,³⁶ A. Sidoti,⁴⁴ P. Sinervo,³³ A. Sisakyan,¹⁴ J. Sjolín,⁴² A. Skiba,²⁵ A.J. Slaughter,¹⁶ K. Sliwa,⁵⁶ J.R. Smith,⁷ F.D. Snider,¹⁶ R. Snihur,³³ M. Soderberg,³⁴ A. Soha,⁷ S. Somalwar,⁵² V. Sorin,³⁵ J. Spalding,¹⁶ M. Spezziga,¹⁶ F. Spinella,⁴⁶ T. Spreitzer,³³ P. Squillacioti,⁴⁶ M. Stanitzki,⁶⁰ A. Staveris-Polykalas,⁴⁶ R. St. Denis,²⁰ B. Stelzer,⁸ O. Stelzer-Chilton,⁴² D. Stentz,³⁸ J. Strologas,³⁷ D. Stuart,¹⁰ J.S. Suh,²⁷ A. Sukhanov,¹⁷ K. Sumorok,³² H. Sun,⁵⁶ T. Suzuki,⁵⁵ A. Taffard,²³ R. Takashima,⁴⁰ Y. Takeuchi,⁵⁵ K. Takikawa,⁵⁵ M. Tanaka,² R. Tanaka,⁴⁰ N. Tanimoto,⁴⁰ M. Tecchio,³⁴ P.K. Teng,¹ K. Terashi,⁵⁰ S. Tether,³² J. Thom,¹⁶ A.S. Thompson,²⁰ E. Thomson,⁴⁵ P. Tipton,⁴⁹ V. Tiwari,¹² S. Tkaczyk,¹⁶ D. Toback,⁵³ S. Tokar,¹⁴ K. Tollefson,³⁵ T. Tomura,⁵⁵ D. Tonelli,⁴⁶ M. Tönnemann,³⁵ S. Torre,¹⁸ D. Torretta,¹⁶ S. Tourneur,⁴⁴ W. Trischuk,³³ R. Tsuchiya,⁵⁷ S. Tsuno,⁴⁰ N. Turini,⁴⁶ F. Ukegawa,⁵⁵ T. Unverhau,²⁰ S. Uozumi,⁵⁵ D. Usynin,⁴⁵ A. Vaiciulis,⁴⁹ S. Vallecorsa,¹⁹ A. Varganov,³⁴ E. Vataga,³⁷ G. Velev,¹⁶ G. Veramendi,²³ V. Veszpremi,⁴⁸ R. Vidal,¹⁶ I. Vila,¹¹ R. Vilar,¹¹ T. Vine,³⁰ I. Vollrath,³³ I. Volobouev,²⁸ G. Volpi,⁴⁶ F. Würthwein,⁹ P. Wagner,⁵³ R. G. Wagner,² R.L. Wagner,¹⁶ W. Wagner,²⁵ R. Wallny,⁸ T. Walter,²⁵ Z. Wan,⁵² S.M. Wang,¹ A. Warburton,³³ S. Waschke,²⁰ D. Waters,³⁰ W.C. Wester III,¹⁶ B. Whitehouse,⁵⁶ D. Whiteson,⁴⁵ A.B. Wicklund,² E. Wicklund,¹⁶ G. Williams,³³ H.H. Williams,⁴⁵ P. Wilson,¹⁶ B.L. Winer,³⁹ P. Wittich,¹⁶ S. Wolbers,¹⁶ C. Wolfe,¹³ T. Wright,³⁴ X. Wu,¹⁹ S.M. Wynne,²⁹ A. Yagil,¹⁶ K. Yamamoto,⁴¹ J. Yamaoka,⁵² T. Yamashita,⁴⁰ C. Yang,⁶⁰ U.K. Yang,¹³ Y.C. Yang,²⁷ W.M. Yao,²⁸ G.P. Yeh,¹⁶ J. Yoh,¹⁶ K. Yorita,¹³ T. Yoshida,⁴¹ G.B. Yu,⁴⁹ I. Yu,²⁷ S.S. Yu,¹⁶ J.C. Yun,¹⁶ L. Zanello,⁵¹ A. Zanetti,⁵⁴ I. Zaw,²¹ F. Zetti,⁴⁶ X. Zhang,²³ J. Zhou,⁵² and S. Zucchelli⁵

(CDF Collaboration)

¹*Institute of Physics, Academia Sinica, Taipei, Taiwan 11529, Republic of China*

²*Argonne National Laboratory, Argonne, Illinois 60439*

³*Institut de Física d'Altes Energies, Universitat Autònoma de Barcelona, E-08193, Bellaterra (Barcelona), Spain*

⁴*Baylor University, Waco, Texas 76798*

⁵*Istituto Nazionale di Fisica Nucleare, University of Bologna, I-40127 Bologna, Italy*

⁶*Brandeis University, Waltham, Massachusetts 02254*

⁷*University of California, Davis, Davis, California 95616*

⁸*University of California, Los Angeles, Los Angeles, California 90024*

⁹*University of California, San Diego, La Jolla, California 92093*

¹⁰*University of California, Santa Barbara, Santa Barbara, California 93106*

¹¹*Instituto de Física de Cantabria, CSIC-University of Cantabria, 39005 Santander, Spain*

¹²*Carnegie Mellon University, Pittsburgh, PA 15213*

¹³*Enrico Fermi Institute, University of Chicago, Chicago, Illinois 60637*

¹⁴*Joint Institute for Nuclear Research, RU-141980 Dubna, Russia*

¹⁵*Duke University, Durham, North Carolina 27708*

¹⁶*Fermi National Accelerator Laboratory, Batavia, Illinois 60510*

¹⁷*University of Florida, Gainesville, Florida 32611*

¹⁸*Laboratori Nazionali di Frascati, Istituto Nazionale di Fisica Nucleare, I-00044 Frascati, Italy*

¹⁹*University of Geneva, CH-1211 Geneva 4, Switzerland*

²⁰*Glasgow University, Glasgow G12 8QQ, United Kingdom*

²¹*Harvard University, Cambridge, Massachusetts 02138*

- ²²*Division of High Energy Physics, Department of Physics, University of Helsinki and Helsinki Institute of Physics, FIN-00014, Helsinki, Finland*
- ²³*University of Illinois, Urbana, Illinois 61801*
- ²⁴*The Johns Hopkins University, Baltimore, Maryland 21218*
- ²⁵*Institut für Experimentelle Kernphysik, Universität Karlsruhe, 76128 Karlsruhe, Germany*
- ²⁶*High Energy Accelerator Research Organization (KEK), Tsukuba, Ibaraki 305, Japan*
- ²⁷*Center for High Energy Physics: Kyungpook National University, Taegu 702-701, Korea; Seoul National University, Seoul 151-742, Korea; and SungKyunKwan University, Suwon 440-746, Korea*
- ²⁸*Ernest Orlando Lawrence Berkeley National Laboratory, Berkeley, California 94720*
- ²⁹*University of Liverpool, Liverpool L69 7ZE, United Kingdom*
- ³⁰*University College London, London WC1E 6BT, United Kingdom*
- ³¹*Centro de Investigaciones Energeticas Medioambientales y Tecnologicas, E-28040 Madrid, Spain*
- ³²*Massachusetts Institute of Technology, Cambridge, Massachusetts 02139*
- ³³*Institute of Particle Physics: McGill University, Montréal, Canada H3A 2T8; and University of Toronto, Toronto, Canada M5S 1A7*
- ³⁴*University of Michigan, Ann Arbor, Michigan 48109*
- ³⁵*Michigan State University, East Lansing, Michigan 48824*
- ³⁶*Institution for Theoretical and Experimental Physics, ITEP, Moscow 117259, Russia*
- ³⁷*University of New Mexico, Albuquerque, New Mexico 87131*
- ³⁸*Northwestern University, Evanston, Illinois 60208*
- ³⁹*The Ohio State University, Columbus, Ohio 43210*
- ⁴⁰*Okayama University, Okayama 700-8530, Japan*
- ⁴¹*Osaka City University, Osaka 588, Japan*
- ⁴²*University of Oxford, Oxford OX1 3RH, United Kingdom*
- ⁴³*University of Padova, Istituto Nazionale di Fisica Nucleare, Sezione di Padova-Trento, I-35131 Padova, Italy*
- ⁴⁴*LPNHE, Universite Pierre et Marie Curie/IN2P3-CNRS, UMR7585, Paris, F-75252 France*
- ⁴⁵*University of Pennsylvania, Philadelphia, Pennsylvania 19104*
- ⁴⁶*Istituto Nazionale di Fisica Nucleare Pisa, Universities of Pisa, Siena and Scuola Normale Superiore, I-56127 Pisa, Italy*
- ⁴⁷*University of Pittsburgh, Pittsburgh, Pennsylvania 15260*
- ⁴⁸*Purdue University, West Lafayette, Indiana 47907*
- ⁴⁹*University of Rochester, Rochester, New York 14627*
- ⁵⁰*The Rockefeller University, New York, New York 10021*
- ⁵¹*Istituto Nazionale di Fisica Nucleare, Sezione di Roma 1, University of Rome "La Sapienza," I-00185 Roma, Italy*
- ⁵²*Rutgers University, Piscataway, New Jersey 08855*
- ⁵³*Texas A&M University, College Station, Texas 77843*
- ⁵⁴*Istituto Nazionale di Fisica Nucleare, University of Trieste/ Udine, Italy*
- ⁵⁵*University of Tsukuba, Tsukuba, Ibaraki 305, Japan*
- ⁵⁶*Tufts University, Medford, Massachusetts 02155*
- ⁵⁷*Waseda University, Tokyo 169, Japan*
- ⁵⁸*Wayne State University, Detroit, Michigan 48201*
- ⁵⁹*University of Wisconsin, Madison, Wisconsin 53706*
- ⁶⁰*Yale University, New Haven, Connecticut 06520*

We present the first measurement of the B_s^0 - \overline{B}_s^0 oscillation frequency Δm_s . We use 1 fb^{-1} of data from $p\overline{p}$ collisions at $\sqrt{s} = 1.96 \text{ TeV}$ collected with the CDF II detector at the Fermilab Tevatron. The sample contains signals of 3,600 fully reconstructed hadronic B_s decays and 37,000 partially reconstructed semileptonic B_s decays. We measure the probability as a function of proper decay time that the B_s decays with the same, or opposite, flavor as the flavor at production, and we find a signal consistent with B_s^0 - \overline{B}_s^0 oscillations. The probability that random fluctuations could produce a comparable signal is 0.2%. Under the hypothesis that the signal is due to B_s^0 - \overline{B}_s^0 oscillations, we measure $\Delta m_s = 17.31^{+0.33}_{-0.18} \text{ (stat.)} \pm 0.07 \text{ (syst.) ps}^{-1}$ and determine $|V_{td}/V_{ts}| = 0.208^{+0.001}_{-0.002} \text{ (exp.)}^{+0.008}_{-0.006} \text{ (theo.)}$.

PACS numbers: 12.15.Ff, 12.15.Hh, 13.20.He, 13.25.Hw, 14.40.Nd

Neutral B mesons ($b\overline{q}$, with $q = d, s$ for $\overline{B}_d^0, \overline{B}_s^0$) oscillate from particle to antiparticle due to flavor-changing weak interactions. The probability density P_+ (P_-) for a \overline{B}_q^0 meson produced at proper time $t = 0$ to decay as a

$\overline{B}_q^0 (B_q^0)$ at time t is given by

$$P_{\pm}(t) = \frac{\Gamma_q}{2} e^{-\Gamma_q t} [1 \pm \cos(\Delta m_q t)],$$

where Δm_q is the mass difference between the two mass eigenstates $B_{q,H}^0$ and $B_{q,L}^0$ [1], and Γ_q is the decay width, which is assumed to be equal for the two mass eigenstates. The mass differences Δm_d and Δm_s can be used to determine the fundamental parameters $|V_{td}|$ and $|V_{ts}|$, respectively, of the Cabibbo-Kobayashi-Maskawa (CKM) matrix [2], which relates the quark mass eigenstates to the flavor eigenstates. This determination, however, has large theoretical uncertainties. A measurement of Δm_s combined with $\Delta m_d = 0.505 \pm 0.005 \text{ ps}^{-1}$ [3, 4] would determine the ratio $|V_{td}/V_{ts}|$ with a significantly smaller theoretical uncertainty, contributing to a stringent test of the unitarity of the CKM matrix. Earlier attempts to measure Δm_s have yielded a lower limit: $\Delta m_s > 14.5 \text{ ps}^{-1}$ [3, 5] at the 95% confidence level (C.L.). Recently the DØ Collaboration reported $17 \text{ ps}^{-1} < \Delta m_s < 21 \text{ ps}^{-1}$ at 90% C.L. [6] using a large sample of semileptonic B_s [7] decays.

In this letter we report a measurement of Δm_s using data from 1 fb^{-1} of $p\bar{p}$ collisions at $\sqrt{s} = 1.96 \text{ TeV}$ collected by the CDF II detector at the Fermilab Tevatron. We begin by reconstructing B_s decays in hadronic ($\overline{B}_s^0 \rightarrow D_s^+ \pi^-$, $D_s^+ \pi^- \pi^+ \pi^-$) and semileptonic ($\overline{B}_s^0 \rightarrow D_s^{+(*)} \ell^- \bar{\nu}_\ell$, $\ell = e$ or μ) decay modes using charged particles only [8]. Using the method of maximum likelihood, we extract the value of Δm_s from the probability density functions (PDFs) that describe the measured time development of B_s mesons that decay with the same or opposite flavor as their flavor at production. The proper decay time for each B_s is calculated from the measured distance between the production and decay points, the measured momentum, and the B_s mass $m_{B_s} = 5.3696 \text{ GeV}/c^2$ [3]. The B_s flavor (b or \bar{b}) at decay is determined unambiguously by the charges of the decay products.

To identify the flavor of the B_s at production, we use characteristics of b quark production and fragmentation in $p\bar{p}$ collisions. At the Tevatron, the dominant b quark production mechanisms produce $b\bar{b}$ pairs. The b and \bar{b} are expected to fragment independently into hadrons. In a simple model of fragmentation, a b quark becomes a \overline{B}_s^0 meson when some of the energy of the b quark is used to produce an $s\bar{s}$ quark pair. The b and the \bar{s} bind to form a \overline{B}_s^0 . The remaining s quark may form a K^- . Similarly, a \bar{b} that becomes a B_s^0 is accompanied by a K^+ . One of the two techniques used to identify the production flavor of the B_s is based on the charge of these kaons (same-side tag). The second technique uses the charge of the lepton from semileptonic decays or a momentum-weighted charge of the decay products of the second b hadron produced in the collision (opposite-side tag).

The hadronic and semileptonic decay modes are com-

plementary. Due to the large branching ratio, the semileptonic decays provide a tenfold advantage in signal rate at the cost of significantly worsened decay-time resolution due to the unmeasured ν momentum. Semileptonic decays dominate the sensitivity to oscillations at lower values of Δm_s . The fully reconstructed hadronic B_s decays have superior decay time resolution, and our large sample of these decays is the unique feature that makes CDF sensitive to much larger values of Δm_s than other experiments.

The CDF II detector [9] consists of a magnetic spectrometer surrounded by electromagnetic and hadronic calorimeters and muon detectors [10]. The key features for this measurement include precision vertex determination provided by the seven-layer double-sided inner silicon strip detector [11, 12] supplemented with a single-sided layer of silicon [13] mounted directly on the beampipe at an average radius of 1.5 cm. The 96-layer outer drift chamber [14] is used for both precision tracking and dE/dx particle identification. Time-of-flight (TOF) counters [15] located just outside the drift chamber are used to identify low momentum charged kaons.

Charm and bottom hadrons are selected using a three-level trigger system that exploits the kinematics of production and decay, and the long lifetimes of D and B mesons. A crucial component of the trigger system for this measurement is the Silicon Vertex Trigger [16], which selects events that contain $\overline{B}_s^0 \rightarrow D_s^+ \pi^-$ and $D_s^+ \pi^- \pi^+ \pi^-$ decays. The trigger configuration used to collect the heavy flavor data sample is described in [17].

To reconstruct \overline{B}_s^0 candidates, we first select D_s^+ candidates. We use $D_s^+ \rightarrow \phi \pi^+$, $K^*(892)^0 K^+$, and $\pi^+ \pi^- \pi^+$, with $\phi \rightarrow K^+ K^-$ and $K^{*0} \rightarrow K^+ \pi^-$; we require that ϕ and K^{*0} candidates be consistent with the known masses and widths [3] of these two resonances. These D_s^+ candidates are combined with one or three additional charged particles to form $D_s^+ \ell^-$, $D_s^+ \pi^-$ or $D_s^+ \pi^- \pi^+ \pi^-$ candidates. The D_s^+ and other decay products of a \overline{B}_s^0 candidate are constrained to originate from a common vertex in three dimensions. For the $K^*(892)^0 K^+$ final state, we remove candidates that are consistent with the decay $D^+ \rightarrow K^- \pi^+ \pi^+$. We use a likelihood technique to identify muons [18] and electrons [19].

Backgrounds are suppressed by imposing a requirement on the minimum transverse momentum p_T [20] of the \overline{B}_s^0 and by requiring that the \overline{B}_s^0 and D_s^+ decay vertices are displaced significantly from the $p\bar{p}$ collision position. We find signals of 3,600 hadronic B_s decays and 37,000 semileptonic B_s decays.

For the hadronic decays, the invariant mass distribution has a signal centered close to $m_{B_s} = 5.3696 \text{ GeV}/c^2$ with a width of 14 to 20 MeV/c^2 , depending on the decay mode. Candidates with masses greater than 5.5 GeV/c^2 are used to construct PDFs for combinatorial background. To remove contributions from $\overline{B}_s^0 \rightarrow D_s^{*+} \pi^-$,

$\overline{B}_s^0 \rightarrow D_s^+ \rho^-$ and semileptonic and other partially reconstructed decays, we require the mass of the decay candidates to be greater than $5.3 \text{ GeV}/c^2$. For semileptonic decays we take into account several background contributions, including B meson decays to two charm mesons and real D_s mesons associated with a false lepton.

The decay time in the B_s rest frame is $t = \kappa[L_T m_{B_s}/p_T]$, where L_T is the displacement of the B_s decay vertex with respect to the primary vertex projected onto the B_s transverse momentum vector. The factor κ corrects for missing momentum in the semileptonic decays ($\kappa = 1$ for hadronic decays). To improve the decay-time resolution, we use event-by-event primary vertex position measurements when computing the B_s vertex displacement. The signal decay-time distribution is modeled with $P(t_i, \sigma_{t_i}) = \varepsilon(t_i) \int \Gamma_s e^{-\Gamma_s t'} \mathcal{G}(t' - t_i, \sigma_{t_i}) dt'$, where t_i is the measured decay time of the i th candidate, Γ_s is the B_s decay width, $\mathcal{G}(x - \mu, \sigma)$ is a Gaussian distribution of the random variable x with mean μ and width σ , and σ_{t_i} is the estimated candidate decay-time resolution. The decay-time efficiency function $\varepsilon(t)$ describes trigger and selection biases on the decay-time distribution and is determined from Monte Carlo simulation. For semileptonic decays, the κ distribution is determined from Monte Carlo simulation and is convoluted with the signal decay-time distribution. The missing transverse momentum from unreconstructed particles in the semileptonic decays is an important contribution to the decay-time resolution. To reduce this contribution and make optimal use of the semileptonic decays, we determine the κ distribution as a function of the invariant mass of the $D_s \ell$ pair, $m_{D_s \ell}$. The r.m.s. width of the κ distribution is 3% (20%) for $m_{D_s \ell} = 5.2 \text{ GeV}/c^2$ ($3.0 \text{ GeV}/c^2$).

We estimate the decay-time resolution σ_{t_i} for each candidate using the measured track parameters and their estimated uncertainties. We calibrate this estimate using a large sample of prompt D^+ mesons [21], which we combine with one or three charged particles from the primary vertex to mimic signal topologies. For hadronic decays the average decay-time resolution is 87 fs, which corresponds to one fifth of an oscillation period at the lower limit on Δm_s (14.5 ps^{-1}). For semileptonic decays, the decay-time resolution is worse due to decay topology and the missing momentum of unreconstructed decay products. For example, at $t = 0$, $\sigma_t = 100 \text{ fs}$ (200 fs) for $m_{D_s \ell} = 5.2 \text{ GeV}/c^2$ ($3.0 \text{ GeV}/c^2$) and increases to $\sigma_t = 115 \text{ fs}$ (380 fs) at $t = 1.5 \text{ ps}$.

The flavor of the B_s at production is determined using both opposite-side and same-side flavor tagging techniques. The effectiveness $Q \equiv \epsilon \mathcal{D}^2$ of these techniques is quantified with an efficiency ϵ , the fraction of signal candidates with a flavor tag, and a dilution $\mathcal{D} \equiv 1 - 2w$, where w is the probability that the tag is incorrect.

Opposite-side tags infer the production flavor of the B_s from the decay products of the b hadron produced from the other b quark in the event. We use lepton (e and

μ) charge and jet charge as tags, building on techniques developed for a CDF Run I measurement of Δm_d [22]. If both lepton and jet-charge tags are present, we use the lepton tag, which has a higher average dilution.

The dilution of opposite-side flavor tags is expected to be independent of the type of B meson that produces the hadronic or semileptonic decay. The dilution is measured in data using large samples of B^- , which do not change flavor, and \overline{B}^0 , which can be used after accounting for their well-known oscillation frequency. The combined opposite-side tag effectiveness is $Q = 1.5 \pm 0.1 \%$, where the uncertainty is dominated by the statistics of the control samples.

Same-side flavor tags [23] are based on the charges of associated particles produced in the fragmentation of the b quark that produces the reconstructed B_s . In the simplest picture of fragmentation, a π^+ (π^-) accompanies the formation of a B^- (B^+), a π^- (π^+) accompanies a \overline{B}^0 (B^0), and a K^- (K^+) accompanies a \overline{B}_s^0 (B_s^0). In Run I, CDF established this method of production flavor identification in measurements of Δm_d [24] and the CP symmetry violating parameter $\sin(2\beta)$ [25]. In this analysis, we use dE/dx [19] and time-of-flight information in a combined particle identification likelihood to identify the kaons associated with B_s production. Tracks close in phase space to the B_s candidate are considered as same-side kaon tag candidates, and the track with the largest kaon likelihood is selected as the tagging track.

The performance of the same-side kaon tag for \overline{B}_s^0 is expected to be different than for B^- and \overline{B}^0 . We predict the dilution using simulated data samples generated with the PYTHIA Monte Carlo [26]. Control samples of B^- and \overline{B}^0 are used to validate the predictions of the simulation. The effectiveness of this flavor tag increases with the p_T of the \overline{B}_s^0 ; we find $Q = 3.5\%$ (4.0%) in the hadronic (semileptonic) decay sample. The fractional uncertainty on Q is approximately 25%. This uncertainty is dominated by the differences between data and simulation for kaons found close in phase space to the \overline{B}_s^0 [27] and for the performance of the same-side kaon tag when applied to B^- .

If both a same-side tag and an opposite-side tag are present, we combine the information from both tags assuming they are uncorrelated. The addition of the same-side kaon tag increases the effective sample statistics by more than a factor of three.

We use an unbinned maximum likelihood fit to search for B_s oscillations. The likelihood combines mass, decay time, decay-time resolution and flavor tagging information for each candidate, and includes terms for signal and each type of background. The fit is done in three stages. First, a combined mass and decay-time fit is performed to separate signal from background and to fix mass and decay-time models. Combined fits for B_s mass and de-

cay width in hadronic samples and for decay width in the semileptonic samples yield measurements consistent with established values [3]. Next, flavor asymmetries are measured for background components. The last step is a fit for $B_s^0 - \bar{B}_s^0$ oscillations; the mass and decay-time models and background asymmetries are fixed from the previous two stages.

The signal PDF has the general form:

$$\mathcal{S}_{\pm}(t_i, \sigma_{t_i}, \mathcal{D}_i) = \varepsilon(t_i) \int \frac{\Gamma_s}{2} e^{-\Gamma_s t'} [1 \pm \mathcal{A} \mathcal{D}_i \cos(\Delta m_s t')] \mathcal{G}(t_i - t', \sigma_{t_i}) dt',$$

where \mathcal{D}_i is the i th candidate dilution, and $t_i, \sigma_{t_i}, \mathcal{G}$, and $\varepsilon(t)$ have been defined previously. Following the method described in [28], we fit for the oscillation amplitude \mathcal{A} while fixing Δm_s to a probe value. When all detector effects ($\mathcal{D}_i, \sigma_{t_i}$) are calibrated, the oscillation amplitude is expected to be consistent with $\mathcal{A} = 1$ when the probe value is the true oscillation frequency, and consistent with $\mathcal{A} = 0$ when the probe value is far from the true oscillation frequency. Figure 1 (upper) shows the fitted value of the amplitude as a function of the oscillation frequency. The sensitivity of the measurement is defined by the maximum value of Δm_s where $\mathcal{A} = 1$ is excluded at 95% C.L. if the measured value of \mathcal{A} were zero. Our sensitivity is 25.8 ps^{-1} and exceeds the combined sensitivity of all previous experiments [3]. At $\Delta m_s = 17.3 \text{ ps}^{-1}$, the observed amplitude $\mathcal{A} = 1.03 \pm 0.28(\text{stat.})$ is consistent with unity, indicating that the data are compatible with $B_s^0 - \bar{B}_s^0$ oscillations with that frequency, while the amplitude is inconsistent with zero: $\mathcal{A}/\sigma_{\mathcal{A}} = 3.7$, where $\sigma_{\mathcal{A}}$ is the uncertainty on \mathcal{A} . The negative amplitudes measured at frequencies slightly below and slightly above the peak frequency are expected and are due to the finite range in signal decay time that is imposed by the trigger and selection criteria. The systematic uncertainty on \mathcal{A} is mainly due to uncertainties on σ_{t_i} and \mathcal{D}_i . Since the effect of these uncertainties on \mathcal{A} and $\sigma_{\mathcal{A}}$ are correlated, the ratio $\mathcal{A}/\sigma_{\mathcal{A}}$ has negligible systematic uncertainty.

The significance of the potential signal is evaluated from $\Lambda \equiv \log[\mathcal{L}^{\mathcal{A}=0}/\mathcal{L}^{\mathcal{A}=1}(\Delta m_s)]$, which is the logarithm of the ratio of likelihoods for the hypothesis of oscillations ($\mathcal{A} = 1$) at the probe value and the hypothesis that $\mathcal{A} = 0$, which is equivalent to random production flavor tags. Figure 1 (lower) shows Λ as a function of Δm_s . A minimal value of $\Lambda = -6.75$ is observed at $\Delta m_s = 17.3 \text{ ps}^{-1}$. The significance of the signal is quantified by the probability that randomly tagged data would produce a value of Λ lower than -6.75 at any value of Δm_s . We repeat the fit 50,000 times with random tagging decisions, and we find this probability is 0.2%.

Under the hypothesis that the signal is due to $B_s^0 - \bar{B}_s^0$ oscillations, we fix $\mathcal{A} = 1$ and fit for the oscillation frequency. We find $\Delta m_s = 17.31_{-0.18}^{+0.33}(\text{stat.}) \pm 0.07(\text{syst.}) \text{ ps}^{-1}$ and the range $17.01 \text{ ps}^{-1} < \Delta m_s <$

17.84 ps^{-1} ($16.96 \text{ ps}^{-1} < \Delta m_s < 17.91 \text{ ps}^{-1}$) at 90% (95%) C.L. All systematic uncertainties affecting \mathcal{A} are unimportant for Δm_s . The only non-negligible systematic uncertainty on Δm_s is from the uncertainty on the absolute scale of the decay-time measurement. Contributions to this uncertainty include biases in the primary-vertex reconstruction due to the presence of the opposite-side b hadron, uncertainties in the silicon-detector alignment, and biases in track fitting. The measured $B_s^0 - \bar{B}_s^0$ oscillation frequency is used to derive the ratio $|V_{td}/V_{ts}| = \xi \sqrt{\frac{\Delta m_d}{\Delta m_s} \frac{m_{B^0}}{m_{B^0}}}$. As inputs we use $m_{B^0}/m_{B^0} = 0.98390$ [29] with negligible uncertainty, $\Delta m_d = 0.505 \pm 0.005 \text{ ps}^{-1}$ [3] and $\xi = 1.21_{-0.035}^{+0.047}$ [30]. We find $|V_{td}/V_{ts}| = 0.208_{-0.002}^{+0.001}(\text{exp.})_{-0.006}^{+0.008}(\text{theo.})$.

In conclusion, we present the first measurement of Δm_s . The precision of this measurement is better than 2%. The value of Δm_s is consistent with standard model expectations [31] and with previous bounds. Our measured value of Δm_s allows us to determine $|V_{td}/V_{ts}|$ with unprecedented precision and can be used to improve constraints on the unitarity of the CKM matrix and on scenarios involving new physics.

We thank the Fermilab staff and the technical staffs of the participating institutions for their vital contributions. This work was supported by the U.S. Department of Energy and National Science Foundation; the Italian Istituto Nazionale di Fisica Nucleare; the Ministry of Education, Culture, Sports, Science and Technology of Japan; the Natural Sciences and Engineering Research Council of Canada; the National Science Council of the Republic of China; the Swiss National Science Foundation; the A.P. Sloan Foundation; the Bundesministerium für Bildung und Forschung, Germany; the Korean Science and Engineering Foundation and the Korean Research Foundation; the Particle Physics and Astronomy Research Council and the Royal Society, UK; the Russian Foundation for Basic Research; the Comisión Interministerial de Ciencia y Tecnología, Spain; in part by the European Community's Human Potential Programme under contract HPRN-CT-2002-00292; and the Academy of Finland.

-
- [1] C. Gay, *Annu. Rev. Nucl. Part. Sci.* **50**, 577 (2000). We set $\hbar = c = 1$ and report $\Delta m_q = m_{B_{q,H}^0} - m_{B_{q,L}^0}$ in inverse picoseconds.
 - [2] N. Cabibbo, *Phys. Rev. Lett.* **10**, 531 (1963); M. Kobayashi and T. Maskawa, *Prog. Theor. Phys.* **49**, 652 (1973).
 - [3] S. Eidelman *et al.*, *Phys. Lett. B* **592**, 1 (2004) and 2005 partial update for the 2006 edition available on the PDG WWW pages (<http://pdg.lbl.gov/>).
 - [4] K. Abe *et al.* (BELLE Collaboration), *Phys. Rev. D* **71**, 072003 (2005); **71**, 079903(E) (2005); N. C. Hast-

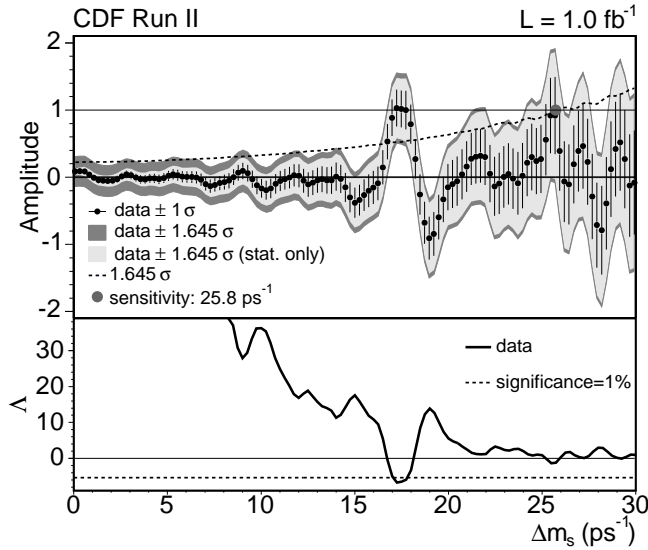


FIG. 1: (Upper) The measured amplitude values and uncertainties versus the $B_s^0-\bar{B}_s^0$ oscillation frequency Δm_s . At 17.3 ps^{-1} , the amplitude is consistent with one and inconsistent with zero at 3.7 standard deviations. Shown in light gray and dark gray are the 95% one-sided confidence level bands for statistical uncertainties only and including systematic uncertainties, respectively.

(Lower) The logarithm of the ratio of likelihoods for amplitude equal to zero and amplitude equal to one, $\Lambda = \log[\mathcal{L}^{A=0}/\mathcal{L}^{A=1}(\Delta m_s)]$, versus the oscillation frequency. The deepest minimum is $\Delta m_s = 17.3\text{ ps}^{-1}$, where $\Lambda = -6.75$. The dashed horizontal line indicates the value of Λ that corresponds to a probability of 1% in the case of randomly tagged data.

ings *et al.* (BELLE Collaboration), Phys. Rev. D **67**, 052004 (2003); B. Aubert *et al.* (BABAR Collaboration), Phys. Rev. Lett. **88**, 221803 (2002).

[5] J. Abdallah *et al.* (DELPHI Collaboration), Eur. Phys. J. C **35**, 35 (2004); K. Abe *et al.* (SLD Collaboration), Phys. Rev. D **67**, 012006 (2003); A. Heister *et al.* (ALEPH Collaboration), Eur. Phys. J. C **29**, 143 (2003).

[6] V. M. Abazov *et al.* (DØ Collaboration), “First direct two-sided bound on the B_s^0 oscillation frequency,” hep-ex/0603029, submitted to Physical Review Letters.

[7] The symbol B_s refers to the combination of \bar{B}_s^0 and B_s^0 decays.

[8] References to a particular process imply that the charge conjugate process is included as well.

[9] D. Acosta *et al.* (CDF Collaboration), Phys. Rev. D **71**, 032001 (2005); R. Blair *et al.* (CDF Collabora-

tion), “The CDF-II Detector Technical Design Report,” FERMILAB-PUB-96-390-E (1996).

[10] A. Abulencia *et al.* (CDF Collaboration), “Measurements of inclusive W and Z cross sections in $p\bar{p}$ collisions at $\sqrt{s} = 1.96\text{ TeV}$,” hep-ex/0508029, submitted to Physical Review D.

[11] A. Sill *et al.*, Nucl. Instrum. Methods Phys. Res., Sect. A **447**, 1 (2000).

[12] A. Affolder *et al.*, Nucl. Instrum. Methods Phys. Res., Sect. A **453**, 84 (2000).

[13] C. S. Hill *et al.*, Nucl. Instrum. Methods Phys. Res., Sect. A **530**, 1 (2004).

[14] T. Affolder *et al.*, Nucl. Instrum. Methods Phys. Res., Sect. A **526**, 249 (2004).

[15] S. Cabrera *et al.*, Nucl. Instrum. Methods Phys. Res., Sect. A **494**, 416 (2002).

[16] W. Ashmanskas *et al.*, Nucl. Instrum. Methods Phys. Res., Sect. A **518**, 532 (2004).

[17] A. Abulencia *et al.* (CDF Collaboration), Phys. Rev. Lett. **96**, 191801 (2006).

[18] G. Giurgiu, Ph. D. thesis, Carnegie Mellon University, 2005, FERMILAB-THESIS-2005-41.

[19] A. Abulencia *et al.* (CDF Collaboration), “Measurement of the B_c^+ Meson Lifetime using $B_c^+ \rightarrow J/\psi e^+ \nu_e$,” hep-ex/0603027, submitted to Physical Review Letters.

[20] The transverse momentum p_T is the magnitude of the component of the momentum perpendicular to the proton beam direction.

[21] D. Acosta *et al.* (CDF Collaboration), Phys. Rev. Lett. **91**, 241804 (2003).

[22] F. Abe *et al.* (CDF Collaboration), Phys. Rev. D **60**, 072003 (1999).

[23] A. Ali and F. Barreiro, Z. Phys. C **30**, 635 (1986); M. Gronau, A. Nippe, J. L. Rosner, Phys. Rev. D **47**, 1988 (1993); M. Gronau and J. L. Rosner, Phys. Rev. D **49**, 254 (1994).

[24] F. Abe *et al.* (CDF Collaboration), Phys. Rev. D **59**, 032001 (1999).

[25] T. Affolder *et al.* (CDF Collaboration), Phys. Rev. D **61**, 072005 (2000).

[26] T. Sjöstrand *et al.*, Computer Phys. Commun. **135**, 238 (2001). We use version 6.216.

[27] D. Usynin, Ph. D. thesis, University of Pennsylvania, 2005, FERMILAB-THESIS-2005-68.

[28] H.G. Moser and A. Roussarie, Nucl. Instrum. Methods Phys. Res., Sect. A **A384**, 491 (1997).

[29] D. Acosta *et al.* (CDF Collaboration) Phys. Rev. Lett. **96**, 202001 (2006).

[30] M. Okamoto, PoS LAT2005 (2005) 013, (hep-lat/0510113).

[31] M. Bona *et al.* (UTfit Collaboration), JHEP **0507** 028 (2005); J. Charles *et al.* (CKMfitter Collaboration), Eur. Phys. J. C **41**, 1 (2005).